Journal of the Nigerian Association of Mathematical Physics
Volume **13 (November, 2008), 391 - 396**

Enhancing refraction statics correction from first break interpretation - the Niger Delta example

***[1]O. Ujuanbi, [1]S. I. Jegede, [2]E. C. Okolie and [3]J. T. Erimafa**
[1]Department of Physics, Ambrose Alli University, Ekpoma, Nigeria
[2]Department of Physics, Delta State University, Abraka, Nigeria
[3]Department of Mathematics, Ambrose Alli University, Ekpoma, Nigeria

Abstract

The focus of this paper is on improving the statics corrections obtained from first break interpretation using generalized linear inversion GLI3D by effective incorporation of uphole data. Different near surface velocity models were compared by computing the corresponding statics and evaluating their impact on seismic image. The results show that to maximise first break interpretation using the generalized linear inversion method, the uphole information regarding the actual number of layers and velocities should be incoporated into the GLI3D scheme so as to allow for faster convergence between the model breaks and the field breaks resulting in better statics application.

1.0 Introduction

High resolution seismic data requires careful data acquisition and processing. The major processing step that influence resolution of land data is statics correction (Harherly et al 1994 [4].

Statics are intended to correct for that data degrading effects of near surface weathering and elevation changes with respect to a defined reference datum

Analysis of refracted arrivals has been the subject of research over the years, and a number of methods have been proposed (Hagedoon, 1959, Morozov *et al* 2007). However, while these methods are very suitable for hand- interpretation of individual records, they tend to suffer from a number of limitations when applied to computer analysis of multi-fold data. These limitations include restrictive assumptions placed on the near-surface model, estimation of the long-wavelength static component only, difficulty in computer automation, sensitivity to errors in the picked arrival times, and inability to use the full redundancy implied in CDP shooting. In order to avoid these limitations Hampson and Russel in 1984, developed a near surface model based on iterative ray tracing which is bane of this work

2.0 Location

The study area covers about 468.5 and 313.1km of surface and subsurface area respectively. It is located within latitude $5^0\ 00^{11}\ 0^1$ and $5^0\ 30^{11}\ 0^1$ and longitude $6^0\ 10^{11}\ 0^1$ and $7^0\ 10^{11}\ 0^1$.

The survey area is characterised by two distinct elevation and physiographic profile as shown in Figure 2.1. The Sambreiro river that flows in the north-south direction and associated flood plain describe a low elevation plain and swampy nature. This low elevation profile is dovetailed with a relatively flat higher topography east of the Sambreiro floodplain by a sharp and steep escarpment. This higher elevation profile has firm and dry land.

3.0 Theory

In the theory of Generalized linear inversion as explained by Backus and Gilbert (1967), a set of model parameters represented by the vector M is choosen,

$$M = (m_1, m_2, ..., m_k)^T.$$

***Corresponding Author**
***e-mail address omiujuanbi@yahoo.com**
We wish to express our profound gratitude to SPDC Nigeria for access to their data used in this work.

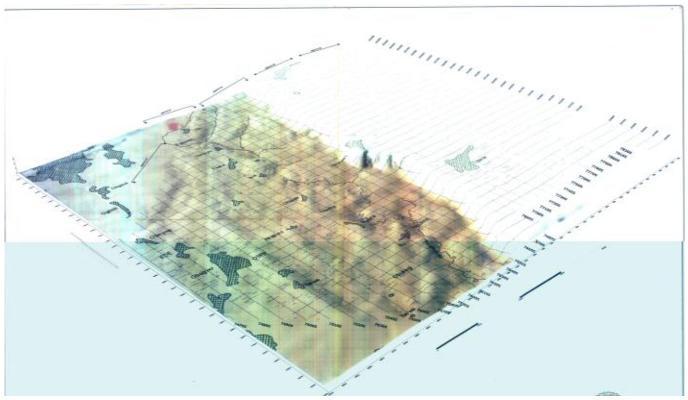

Figure 2.1: Location map

The model parameters are assumed to yield a set of observations represented by the vector

$$T = (t_1, t_2,, ..., t_n)^T$$

Through some non linear functional relationship, A: such that

$$t_i = A_i(m_1, m_2, \ldots, .m_k),\ i = 1, 2, \ldots, n$$

In this particular problem, the vector *M* is the set of all the unknown thicknesses and velocities in the near surface model, the vector T is the set of all observed first breaks, and the operator *A* is ray tracing algorithm incorporating Snell's law. Starting from an initial model guess, *M*, a set of arrival times is calculated and compared with measured arrivals of which there is always a residual error between the observed and the model breaks. The Generalized linear inverse method reduces to analyzing this residual error vector to determine a set of corrections to the model.

In the General iterative modelling algorithm as shown in Figure 3.1 the user inputs an initial guess as to the near-surface configuration which tells the program how many layers are expected and their approximate velocities and thicknesses. The program performs a series of iterations in which the model breaks are calculated by ray- tracing and compared with the measured breaks calculated. This procedure is repeated until some acceptable correspondence is reached between observed and model breaks. Although both velocities and depths may vary with each station, the algorithm can be more robust by forcing a more slowly varying model. It is also expected that the **correct number of layers** must be specified and that the geology must vary slowly enough for ray tracing to be effective. Secondly the initial guess must be close enough to the correct answer to allow convergence within a reasonable number of iterations. Thirdly, the input first break picks must be free of errors.

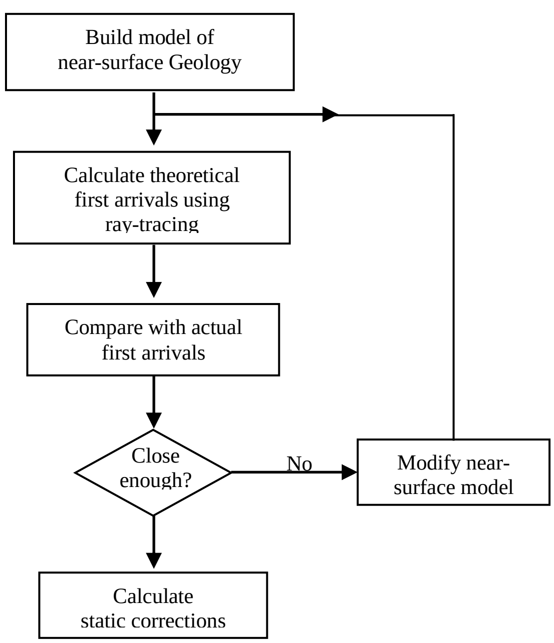

Figure 3.1: Refraction analysis by generalized linear inversion from Hampson and Russel 1984

4.0 Data acquisition

4.1 Weathering survey

The weathering layers were determined using the low velocity layer (LVL) and uphole surveys respectively. The aim was to estimate near surface velocities and layer depths at discrete locations along a seismic line, so as to generate a near surface model by interpolating velocities and layer depths along the seismic lines.

The uphole/LVL (refraction) survey was carried out in 36 locations on a grid of 4 × 4 sq.km as shown in Figure 4.1. However some 19 points were 'offsetted' or moved from the planned grid position by a maximum of a receiver or source line due to access difficulties. The upholes were acquired with generally fair quality with an average well depth of 60m.

To make an accurate estimation of the statics from the uphole data a method known as Replacement Statics was used. The effect is to remove both the effect of the elevation difference and the effect of all the weathering layers. In doing this a simple equation was derived for this computation as

$$T = D_0/V_0 + D_1/V_1 + (D_0 + D_1 + E)/V_2 \qquad (4.1)$$

where D_0 is the depth of the weathering layer, D_1 is the depth of the subweathering layer, V_0 the velocity of the first layer, V_1 = the velocity of the second layer and V_2= the consolidated layer velocity

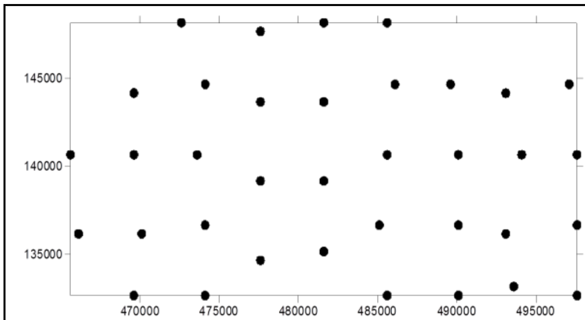

Figure 4.1: Uphole locations

5.0 Results

The uphole and LVL result for the entire prospect as well as the computed statics for each location is shown in table 1.With the available uphole data for this prospect the average velocity of the first layer was found to be 340m/s

Secondly, from uphole/LVL survey two layer earth models was clearly delineated as against the oversimplified generally assumed 1 layer model for prospects within the Niger-Delta.

Thus in the GLI3D program, the following earth models were tested

- 2 layer model with first layer velocity of 340m/s (Model 1)
- 2 layer model with first layer velocity of 650m/s (Model 2)
- layer model with first layer velocity of 650m/s (Model 3)

The result of statics computation using the GLI3D iterative scheme for the three special model examples at the various uphole locations is shown in table 2.

6.0 Discussion of results

From this Table 5.2, it can be easily seen that the static results of model 1 example has a closer relationship to the statics result obtained from uphole data which in this case is the control. This is closely followed by model 3 with model 2 being the least correlated. This is also expressed by the wireframe view of the different models.

Although model 1 and model 3 results are close in their statics values, as well as the wireframe representation, model 1 appears to have a closer relationship with the computed statics from uphole data.

The right hand section of figure 6.1 shows the brut stack obtained by stacking the few shots, and the left side of the section shows the stacked section of the shots after refraction statics have been applied using model 1. Figure 6.2 is a compared stack sections after statics application using model 1 as shown on the left hand side of the figure and with model 2 on the right hand side. Figure 6.3 is a compared stack sections after statics application using model 1 and model 3 respectively.

S/N	SHOT LOCATION	SHOT DEPTH	X	Y	Z	D_0	D_1	V_0	V_1	V_2	STATICS
1	35085/74905	60	465603.34	140644.11	14.690	1.400	30.70	219	1364	2005	-20.216734
2	34185/75005	60	466103.91	136143.26	13.320	1.500	22.00	240	1298	1786	-17.499265
3	33485/75705	60	469603.50	132643.26	11.320	1.600	35.70	447	1541	1817	-12.447899
4	35085/75705	60	469602.73	140644.63	11.240	2.700	35.30	678	1665	2140	-12.678829
5	35785/75705	60	469604.12	144144.42	13.800	2.000	26.30	358	1475	1916	-15.849251
6	33485/76605	60	474103.21	132643.54	31.790	3.000	19.30	276	621	1747	-47.38064
7	33885/77305	60	477603.68	134644.28	30.870	4.700	11.40	218	817	2208	-42.202433
8	35685/77305	1	477604.05	143645.66	36.740	1.700	16.40	200	503	1750	-51.755802
9	36485/77305	60	477603.78	147643.06	36.550	1.300	19.40	199	722	1760	-42.408151
10	34785/77305	1	477603.94	139143.04	33.100	1.700	13.90	264	475	1667	-46.200452
11	33985/78105	60	481605.39	135143.55	36.520	2.600	17.40	265	673	1712	-45.315237
12	35685/78105	1	481603.51	143643.56	40.200	1.300	15.30	225	425	1735	-55.380083
13	34785/78105	1	481603.57	139143.80	38.600	1.300	14.90	205	450	1680	-52.785908
14	36585/78105	60	481603.59	148143.43	42.770	2.200	19.00	265	658	1783	-49.274855
15	36585/78905	60	485604.13	148143.94	44.450	2.200	18.10	256	635	1807	-50.46238
16	35885/79005	60	486103.30	144637.50	44.500	1.500	19.50	290	634	1767	-49.228889
17	34285/78805	60	485104.00	136642.90	37.900	3.800	16.40	324	681	1770	-45.810627
18	34285/79805	60	490104.16	136643.96	39.930	2.100	15.20	252	630	1610	-46.516218
19	33485/79805	60	490102.97	132643.74	37.600	2.600	12.80	233	659	1721	-43.481644
20	35085/78905	60	485604.20	140643.00	40.500	2.200	17.60	290	649	1756	-46.493006
21	33485/78905	1	485603.00	132643.60	36.100	3.400	14.00	300	603	1670	-45.748185
22	35885/79705	60	489604.53	144643.44	44.390	2.200	19.90	291	704	1742	-48.62282
23	35085/79805	60	490103.55	140643.81	40.840	4.300	17.70	302	816	1784	-46.490125
24	35785/80405	60	493103.63	144143.14	44.070	2.500	13.90	286	646	1670	-46.827149
25	35085/81305	60	497604.23	140643.99	43.600	2.100	13.90	224	616	1759	-47.630668
26	35885/81205	60	497103.61	144643.87	47.440	2.800	17.60	313	630	1803	-51.879422
27	33585/80505	60	493603.60	133143.60	37.500	3.100	21.90	322	939	1998	-39.206269
28	33485/81305	60	497603.95	132643.40	39.500	2.100	18.10	374	710	1721	-42.322341
29	34285/81305	1	497603.89	136641.49	42.400	2.500	14.70	255	565	1680	-50.821621

30	35085/80605	60	494103.42	140643.65	41.090	2.000	13.50	248	660	1764	-43.025864
31	34185/80405	60	493102.50	136142.56	39.260	2.300	13.40	301	607	1712	-43.478661

Table 5.1: Uphole data with the compound statics

Note that the effect of the statics application is more obvious in the stacked section not only in the time shift but in the continuity of events. Despite the scanty nature of shots as used in this investigation, model 1 application provides flatter structures and better continuity of events(i.e the major events at 900ms and 1400ms), so it is likely to approximate the earth's complexities better. At the left border, the time difference between the reflection at 500ms exceeds about 10ms.

The two layer model driven approach with uphole information looks the best in terms of signal coherence from the few shots examined. This means that changes in shallow layer thickness are not less relevant than elevation discontinuities. From all the display above it is obvious that the improvement due to the incoporation of uphole information to the GLI information is very impressive- far beyond what one would expect with the general known assumption of known geology of the area. Thus, there is always the need for practical, efficient integration of uphole information into 3D near surface modeling so as to obtain optimum statics correction.

Table 5.2: Statics results for the three model examples

S/N	SHOT LOCATION	X	Y	Z	UPHOLE STAT	MODEL1	MODEL 2	MODEL3
1	35085/74905	465603.34	140644.11	14.690	-20.200	-18.00	-16.00	-19.00
2	34185/75005	466103.91	136143.26	13.320	-17.500	-12.00	-15.00	-9.00
3	33485/75705	469603.50	132643.26	11.320	-12.400	-7.00	-6.00	-6.00
4	35085/75705	469602.73	140644.63	11.240	-12.700	-21.00	-19.00	-16.00
5	35785/75705	469604.12	144144.42	13.800	-15.800	-10.00	-11	-10
6	33485/76605	474103.21	132643.54	31.790	-47.300	-38.00	-32	-38
7	33885/77305	477603.68	134644.28	30.870	-42.200	-31.00	-35	-31
8	35685/77305	477604.05	143645.66	36.740	-51.800	-41.00	-41	-42
9	36485/77305	477603.78	147643.06	36.550	-42.400	-43.00	-42	-42
10	34785/77305	477603.94	139143.04	33.100	-46.200	-34.00	-37	-38
11	33985/78105	481605.39	135143.55	36.520	-45.300	-41.00	-37	-39
12	35685/78105	481603.51	143643.56	40.200	-55.300	-45.00	-43	-45
13	34785/78105	481603.57	139143.80	38.600	-52.800	-46.00	-43	-45
14	36585/78105	481603.59	148143.43	42.770	-49.300	-49.00	-47	-48
15	36585/78905	485604.13	148143.94	44.450	-50.400	-44.00	-42	-44
16	35885/79005	486103.30	144637.50	44.500	-49.200	-46.00	-43	-47
17	34285/78805	485104.00	136642.90	37.900	-45.800	-38.00	-36	-36
18	34285/79805	490104.16	136643.96	39.930	-46.800	-37.00	-29	-39
19	33485/79805	490102.97	132643.74	37.600	-43.500	-38.00	-32	-38
20	35085/78905	485604.20	140643.00	40.500	-46.500	-44.00	-42	-43
21	33485/78905	485603.00	132643.60	36.100	-45.700	-37.00	-35	-36
22	35885/79705	489604.53	144643.44	44.390	-48.600	-48.00	-46	-48
23	35085/79805	490103.55	140643.81	40.840	-46.500	-39.00	-36	-41
24	35785/80405	493103.63	144143.14	44.070	-46.800	-43.00	-40	-43
25	35085/81305	497604.23	140643.99	43.600	-47.600	-46.00	-42	-48
26	35885/81205	497103.61	144643.87	47.440	-51.900	-46.00	-43	-48
27	33585/80505	493603.60	133143.60	37.500	-39.200	-38.00	-36	-38
28	33485/81305	497603.95	132643.40	39.500	-42.300	-49.00	-45	-49
29	34285/81305	497603.89	136641.49	42.400	-50.800	-43.00	-40	-43
30	35085/80605	494103.42	140643.65	41.090	-43.000	-41.00	-34	-43
31	34185/80405	493102.50	136142.56	39.260	-43.500	-37.00	-33	-37
32	34185/75805	470103.72	136144.20	11.480	-8.700	-10.00	-11	-10
33	36585/76405	472603.12	148147.33	12.020	-8.300	-7.00	-6	-6
34	35085/76505	473602.77	140639.76	12.260	-8.600	-7.00	-8	-9
35	35885/76605	474104.41	144646.86	14.120	-11.900	-12.00	-11	-12
36	34285/76605	474102.01	136643.23	12.100	-8.700	-5.00	-4	-7

Figure 5.1 shows the wireframe plot of the computed statics from uphole data. The plots of the statics computed from the three model examples are shown in figures 5.2 to 5.4 respectively.

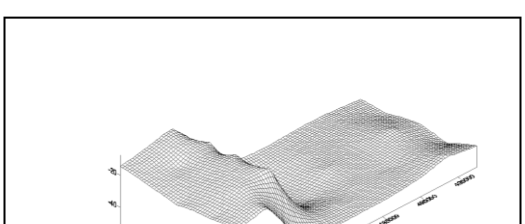

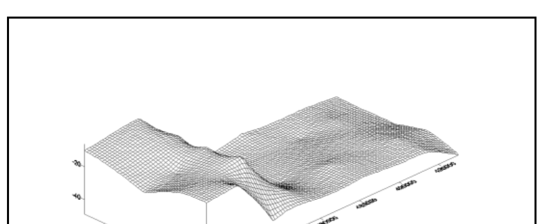

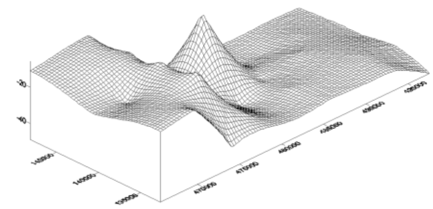

Figure 5.3: 3D view of computed statics from refraction breaks using model 2

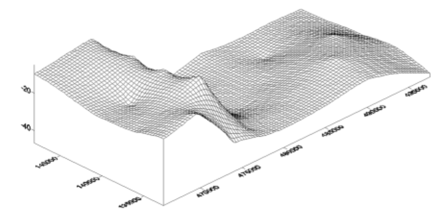

Figure 5.4: 3D view of computed statics from refraction breaks using model 3

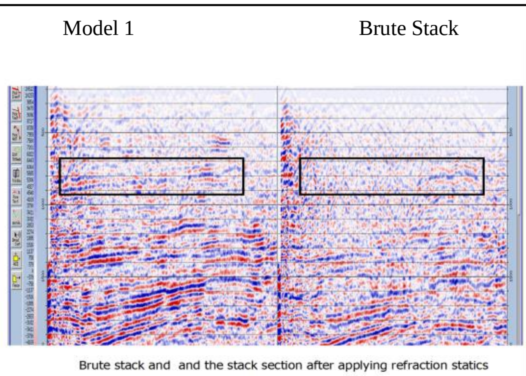

Figure 6.1: Compared sections of brute stack and statics application using models 1

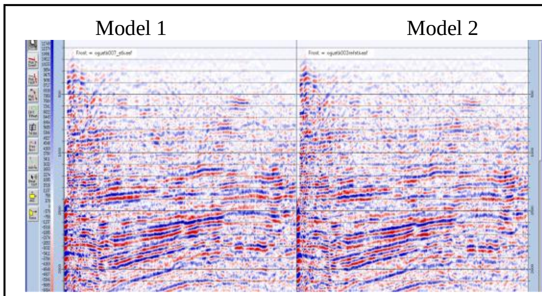

Comparison between stack sections after applying refraction statics using model 1 and model 2.

Figure 6.2: Compared sections of statics application using models 1 and 2

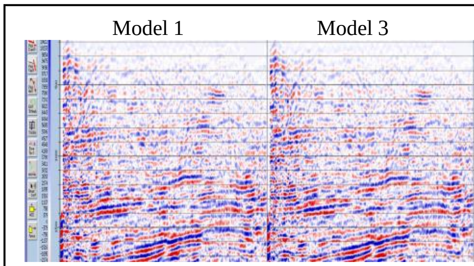

Comparison between stack sections after applying refraction statics using model 1 and model 3

Figure 6.3: Compared sections of statics application using models 1 and 3

7.0 Conclusion

From the sample density of 36 uphole points, the average velocity of the first refractor is 668m/s and the second refractor consolidated layer was evaluated to be 1790m/s. From the calculated variables of the various layers, contour maps were generated which provide some measure of surface trend, although the volume of data control points is insufficient for a conclusive trend analysis. The GLI3D solution of the refraction breaks has been found to be reliable in surface trend analysis in view of the volume and density of the data. However, this work has shown that to maximise its usefulness the uphole information regarding the actual number of layers and velocities should be incoporated into the GLI3D scheme so as to allow for faster convergence between the model breaks and the field breaks resulting in better statics application. This work has further confirmed that calibration by sparse upholes is necessary, but often insufficient to obtain the resolution needed. The major differences observed in our data set were due to the number of layers for our shallow earth model

References

[1] Backus, G. E and Gilbert. J .F 1967. Numerical application of a formalism for geophysical inverse problems: Geophysical Journal, Vol 13 P 247-276.

[2] Hagedoorn, J. G., 1959. The plus-minus method of interpreting seismic refraction sections, Geophys. Prosp., 7, 158-182.

[3] Hampson, D. and Russel, B., 1984. First break interpretation using generalized linear inversion, J. Can. Soc. Expl. Geophys.,20, No1, pp 40-54.

[4] Hatherly, P.J., Urosevic, M., Lambourne, A. and Evans, B. J., 1994. Simple approach to calculating refraction statics corrections (short note): Geophysics, Soc. Of Expl. Geophys., 59, 156-160.

[5] Morozov, I., Reilkoff, B., and Chubak, G., 2007. A generalized web service model for geophysical data processing and modeling, Computers & Geosciences, 32, 1403-1410.